Carbohydrate Polymers 250 (2020) 116983

Contents lists available at ScienceDirect

Carbohydrate Polymers

journal homepage: www.elsevier.com/locate/carbpol

Rapid synthesis of chitosan-capped gold nanoparticles for analytical application and facile recovery of gold from laboratory waste

Thana Thanayutsiri [a], Prasopchai Patrojanasophon [a], Praneet Opanasopit [a], Tanasait Ngawhirunpat [a], Samawadee Plianwong [b], Theerasak Rojanarata [a,*]

[a] Pharmaceutical Development of Green Innovations Group (PDGIG), Faculty of Pharmacy, Silpakorn University, Nakhon Pathom 73000, Thailand
[b] Faculty of Pharmaceutical Sciences, Burapha University, Chonburi 20131, Thailand

ARTICLE INFO

Keywords:
Chitosan
Gold nanoparticles
Microwave
Assay
Waste treatment

ABSTRACT

Chitosan-capped gold nanoparticles (CS-AuNPs) were synthesized via a rapid method by exposing 0.75 mL of 10 mM $HAuCl_4$ and 5 mL of 0.1% w/v chitosan solution to microwave irradiation at 125 °C for 40 s. The resulting red colloidal solution contained monodispersed, spherical, and stable CS-AuNPs with a mean diameter of 17.8 nm and showed the maximum absorption peak at 520 nm. Owing to the positively charged surface, CS-AuNPs were applied to the assay of the polyanionic compound disodium edetate based on the aggregation-induced red-to-blue color change of the particles and the measurement of increased absorbance at 670 nm. The assay was accurate and precise; its results were comparable to those obtained from the titrimetric reference method. Moreover, gold was shown to be easily recovered from CS-AuNPs through alkaline-induced precipitation followed by acid treatment and heating, which provides a facile and efficient means for treatment of laboratory waste.

1. Introduction

A large number of studies have been conducted on the applications of gold nanoparticles (AuNPs) in diverse fields, including chemistry, electronics, engineering, and biomedical and pharmaceutical sciences (Akshaya et al., 2020; Kalimuthu, Cha, Kim, & Park, 2020; Liu & Liu, 2019). Likewise, attempts have been made to develop more efficient synthesis routes to obtain gold-based nanomaterials with desirable properties. Among the various fabrication approaches, environmentally friendly processes that require nontoxic precursors and mild reaction conditions, consume less energy, and generate minimal waste are safe, economical, relatively fast, and environmentally sustainable; thus, they have received much attention. These greener synthesis methods include the use of reducing and stabilizing agents that are naturally derived from plants (Khan, Ullah, Khan, Mashwani, & Nadhman, 2019; Santhoshkumar, Rajeshkumar, & Venkat Kumar, 2017; Teimouri et al., 2018), microorganisms (Bu et al., 2019; Patil & Kim, 2018), and biocompatible and renewable compounds (Augustine & Hasan, 2020). In addition, microwave irradiation, which is considered to be a greener means of heating, has been employed in the synthesis of AuNPs, expediting the preparation process and saving cost and energy (El-Naggar, Shaheen, Fouda, & Hebeish, 2016; Kumari, Reddy, & Mittapalli, 2020; Morad, Karim, Altass, & Khder, 2019).

Carbohydrates as monosaccharides and polysaccharides are well-recognized naturally abundant biomolecules that can act as promising candidates for the preparation of metal nanoparticles, owing to their reducing and stabilizing capabilities. Au-NPs have been synthesized using various types of carbohydrates, including glucose (Suvarna et al., 2017), sucrose (Shrivas et al., 2018), carrageenan oligosaccharide (Chen et al., 2018), dextran (Lim et al., 2012), starch (Wongmanee, Khuanamkam, & Chairam, 2017), fucoidan (Kim et al., 2017), agarose (Kattumuri et al., 2006), pectin (Devendiran et al., 2016), and gellan gum (Dhar et al., 2011). In addition, chitosan, which is an aminated polysaccharide consisting of β-1,4 linked residues of N-acetyl glucosamine and glucosamine units, has been utilized for this purpose. From an environmental viewpoint, chitosan is a green polymer because it is naturally produced and derived from the renewable material chitin, which is present in the exoskeletons of crustaceans. Moreover, it is nontoxic and biodegradable. Several studies have revealed that chitosan can reduce the precursor Au(III) to zero-valent AuNP via charge transfer from polar functional groups, i.e., hydroxyl or amino groups (Huang & Yang, 2004). Moreover, the electrostatic forces between the

* Corresponding author at: Faculty of Pharmacy, Silpakorn University, Nakhon Pathom 73000, Thailand.
E-mail address: rojanarata_t@su.ac.th (T. Rojanarata).

https://doi.org/10.1016/j.carbpol.2020.116983
Received 20 May 2020; Received in revised form 11 August 2020; Accepted 20 August 2020
Available online 26 August 2020

tetrachloroaurate ions ($AuCl_4$-) in the solution and the amino groups in chitosan play an important role in the stabilization and formation of AuNPs (Potara, Maniu, & Astilean, 2009); thus, chitosan can act both as a reducing agent and a stabilizing agent for AuNP synthesis. Recently, chitosan-capped AuNPs (CS-AuNPs) have been fabricated and utilized for various applications, such as carriers for drug and gene delivery (Abrica-González et al., 2019; Manivasagan, Bharathiraja, Bui, Lim, & Oh, 2016), functional nanomaterials for cancer phototherapy (Salem, Sliem, El-Sesy, Shouman, & Badr, 2018), colorimetric sensors (Chen, Wang, Chen, Xu, & Liu, 2013; Jiang et al., 2017), and contrast agents for cell and tumor imaging (Sun, Ahn, Kim, & Emelianov, 2019).

When unmodified chitosan is employed for the synthesis of CS-AuNPs without the introduction of any additional reducing agents or capping agents such as sodium citrate or sodium borohydride, conventional heating is mostly used. This method involves heating a mixture of tetrachloroauric acid and chitosan solution under vigorous stirring at the proper temperature, ranging from 70 to 140 °C; the temperature depends on several factors such as the concentrations of chitosan and gold salt, ratio of reactants, and pH of reaction, which are different in each study. Despite the simplicity of the method, the synthesis of CS-AuNPs using conventional heating is time- and energy-consuming, usually requires 15–120 min (Jiang et al., 2017; Martínez-Torres et al., 2018; Mohan, Gunasekaran, & Ravishankar, 2019; Rovais et al., 2018; Sonia, Komal, Kukreti, & Kaushik, 2018; Sun et al., 2017). Compared with conventional heating, microwave irradiation is a more efficient heating method since it not only reduces overall energy consumption but also increases the reaction rates and improves the product uniformity. Currently, many microwave-assisted synthesis methods of gold nanostructured materials, including AuNPs, have been developed (Madhavan, Gangadharan, Ajayan, Chandran, & Raveendran, 2019). In several studies on the synthesis of CS-AuNPs, a one-pot mixture of tetrachloroauric acid and chitosan solution was irradiated with microwave, usually using constant power (watt) set at the appropriate level (Fan, Li, Zhao, Chen, & Li, 2008; Komalam et al., 2012). The results from these studies demonstrated that the time required for the synthesis was significantly shortened to 1–3 min.

To the best of our knowledge, there is no report on the microwave-assisted synthesis of CS-AuNPs in a fixed temperature mode; that is, the temperature is constant throughout the synthesis, and the microwave source itself controls the power delivered to the reactor. To fill this research gap, the aim of this work was to investigate the optimal synthesis protocol in this mode to offer a novel alternative route to the fabrication of CS-AuNPs. Since CS-AuNPs are positively charged owing to chitosan being the capping agent, they were subsequently utilized as a colorimetric sensor for the quantitative determination of the anionic compound ethylenediaminetetraacetic acid disodium salt (Na_2EDTA); this compound is an intravenous chelating agent used for treating heavy metal poisoning and lowering the serum calcium levels in hypercalcemia. The current assay for Na_2EDTA injection, according to the United States Pharmacopeia (USP), is based on a titrimetric method that consists of several steps (USP43-NF38, 2020). The novel analytical method developed in this work would provide a simpler assay, suitable for the analysis of multiple samples. Lastly, the study was also undertaken with the objective of investigating an effective means of laboratory waste treatment. For the first time, it was found that gold could be easily recovered from CS-AuNPs, highlighting a unique and environmentally friendly feature of this nanomaterial.

2. Materials and methods

2.1. Chemicals

Tetrachloroauric acid trihydrate or gold (III) chloride trihydrate ($HAuCl_4{\cdot}3H_2O$), chitosan (low molecular weight of 50,000-190,000 Da, 75%–85% degree of deacetylation), and Na_2EDTA dihydrate were purchased from Sigma-Aldrich (USA). All other chemicals were of analytical grade. Distilled water was used throughout the work. Prior to use for the synthesis of CS-AuNPs, all glassware was cleaned using freshly prepared aqua regia solution ($HCl:HNO_3$, 3:1) and then rinsed thoroughly with water. Commercial edetate disodium injection was used as the sample for the assay. Each ml of the injection contained 150 mg anhydrous Na_2EDTA in water, and the solution contained no bacteriostatic or antimicrobial agent. The solution pH was approximately 7.0 as a result of pH adjustment with sodium hydroxide.

2.2. Microwave-assisted synthesis of CS-AuNPs

To synthesize the CS-AuNPs, first 0.75 mL of 10 mM $HAuCl_4$ solution was added to 5 mL of 0.1%(w/v) chitosan solution prepared in 1%(v/v) acetic acid in a 10 mL reaction vessel. Subsequently, the mixture was placed in a microwave synthesizer (Discover SP, CEM Corporation, USA) and irradiated with microwave; the synthesizer operated in a fixed temperature mode, and the initial ramp time (i.e., the time taken to raise the temperature from ambient to the set level) was 1 min. To establish the optimal protocol for the synthesis, the effects of heating, including temperature and heating time, were investigated by varying the temperature set-points at 105, 125 and 145 °C and the reaction time at 20, 40, and 60 s. After the microwave irradiation, the resulting colloidal gold solutions were rapidly cooled by immersing the reaction vessels in an ice bath to stop the reaction. Finally, the CS-AuNPs were stored at 4 °C in a refrigerator until further use.

2.3. Characterization of CS-AuNPs

The physical appearance, i.e., the color and clarity of the CS-AuNPs solution, was visually examined, and the colloidal property was confirmed by Tyndall effect, a light scattering phenomenon inherent to colloidal systems when a laser beam is passed through the sample solutions. Ultraviolet–visible (UV–vis) spectra were recorded (400–800 nm), using a multimode plate reader (Victor Nivo, PerkinElmer, USA), to determine the surface plasmon resonance bands. For chemical characterization, the CS-AuNPs solution was centrifuged by the Microfuge 16 (Beckman Coulter, USA) at 14,800 rpm for 10 min. After the supernatant was discarded, the precipitate of CS-AuNPs was washed with water, dried at 50 °C overnight, and subjected to Fourier-transform infrared (FTIR) analysis by the KBr disc method using the Thermo Nicolet Nexus 4700 FTIR spectrometer (Thermo Fisher Scientific, USA). The spectra of CS-AuNPs and native chitosan were recorded and compared. For ^{1}H-NMR spectroscopic analysis, chitosan and CS-AuNPs samples were dispersed in 2% acetic acid-d_4 in deuterium oxide (D_2O, chemical shifts (δ) = 4.80 ppm). A 300 MHz NMR spectrometer Bruker AVANCE III HD (Billerica, MA, USA) was used for the analysis at 298 K. The signals were recorded and reported in part per million (ppm) using D_2O as a solvent reference.

The viscosity of sample solutions was analyzed using a Brookfield DV2T viscometer (Middleboro, MA, USA). The sample (30 mL) was prepared in a 50-mL conical tube and measured with a LV-01 spindle at the rotating speed of 200 rpm. The measurement was carried out at controlled temperature of 25 °C.

The morphology and particle size of CS-AuNPs were studied by transmission electron microscopy (TEM). Zetasizer Nano-ZS (Malvern Instruments, UK) was used to measure the hydrodynamic diameter and zeta potential of the nanoparticles. For this purpose, the freshly prepared CS-AuNPs solution was diluted (1:9) with purified water prior to the analysis, which was carried out at 25 °C.

2.4. Development of the assay for Na2EDTA injection using CS-AuNPs

2.4.1. General protocol for the assay

A series of standard solutions of Na_2EDTA (0.1, 0.2, 0.4, 0.6, 0.8, and 1.0 mM) was prepared by dissolving standard Na_2EDTA dihydrate powder in water and diluting with the same solvent at the desired

concentrations. A sample solution was prepared by diluting edetate disodium injection (150 mg Na_2EDTA per mL, equivalent to about 446 mM) with water to obtain a 0.5 mM solution.

The assay was conducted in a 96-well microtiter plate by sequentially adding 25 μL of Britton-Robinson buffer (pH 4), 75 μL of a standard or sample solution of Na_2EDTA, and 100 μL of the as-prepared CS-AuNPs solution. The reaction mixture was thoroughly mixed by repeatedly pipetting up and down and was then kept at room temperature for another 10 min. Afterward, the absorbance of the mixture was measured at 650 nm using a microtiter plate reader. The amount of Na_2EDTA in sample was determined against a four-parameter logistic standard curve of Na_2EDTA in the range of 0.1–1.0 mM.

$$y = \min + \frac{(\max - \min)}{1 + \left(\frac{x}{EC_{50}}\right)^{-Hillslope}}$$

where y is the absorbance at 670 nm and x is the concentration of Na_2EDTA (mM); min = 0.0910, max = 1.2792, EC_{50} = 0.6386, and Hillslope = 2.3777 (coefficient of determination R^2 = 0.9992).

2.4.2. Method validation and comparison with the reference method

To ascertain the analytical performance of the proposed CS-AuNPs-based assay, the assay was validated following the International Conference of Harmonization (ICH) guidelines (ICH Q2 (R1) (2005)). The effective analytical range in which concentration (independent variable) showed a relationship with instrument response (dependent variable) was investigated by fitting the standard curve of Na_2EDTA (0.1–1.0 mM) to an appropriate regression model and calculating the coefficient of determination (r^2). From the regression equation, the limit of detection (LOD) and limit of quantitation (LOQ), defined as 3.3 and 10 times the standard deviation of the Y-intercept divided by the slope, respectively, were determined. The accuracy was evaluated by performing the assays of standard solutions of Na_2EDTA with three known concentration levels (n = 3 for each level), and the percent recovery values (i.e., assayed amount / known amount × 100) were calculated. The intra-day and inter-day precision were studied by analyzing the injection samples in six runs within a day and across three consecutive days, respectively. The variations in assay results were expressed as the relative standard deviation (%RSD) values of the replicates. Finally, the proposed method was applied to the assay of commercial edetate disodium injection, and the analysis results expressed as the percentage of labeled amount were compared with those determined using the USP 42 reference method.

2.5. Recovery of gold and composition analysis

Sodium hydroxide solution (3 M) was added to the colored liquid laboratory waste while stirring until the pH of the mixture rose to about 7, and most CS-AuNPs present in the waste solution were aggregated and precipitated out. After centrifugation at 8,000 x g for 10 min, the mixture apparently separated into the precipitate and a colorless supernatant, which could be discharged. To further recover high-purity gold from CS-AuNPs, the precipitate obtained from the previous step was placed in a porcelain evaporating dish and then dried at room temperature or with the aid of a hot-air oven. Subsequently, to digest and remove organic matter, the dried precipitate was acidified with a few drops of concentrated sulfuric acid and heated using a burner until white fume no longer evolved, after which the gold was obtained as tiny grains.

The elemental composition of the laboratory-recovered gold was analyzed using scanning electron microscopy (SEM, Tescan Mira3) coupled with energy-dispersive X-ray spectroscopy (EDS, Element EDS System, EDAX). These techniques provided information on both the identity and purity of gold in the samples. For the analysis, the gold grain was mounted on the sample stub by double-sided carbon adhesive tape.

2.6. Statistical analysis

Unless otherwise mentioned, experiments were carried out in triplicate, and data were expressed as mean ± standard deviation. Statistical analyses, including Student's *t*-tests, were performed using Microsoft Excel, where a p-value of ≤ 0.05 was considered significant.

3. Results and discussion

3.1. The optimal condition for the microwave-assisted synthesis of CS-AuNPs

The heating temperature has been reported to affect the yield and property of AuNPs synthesized by conventional heating (Latif et al., 2018; Tran, DePenning, Turner, & Padalkar, 2016), and it is carefully controlled during the reaction process. However, for microwave-based synthesis, this parameter has been given less attention and has not been studied as widely as the irradiation power (watts). Therefore, the aims of this work were to investigate the effect of the reaction temperature on the microwave-assisted fabrication of CS-AuNPs and to optimize this parameter for the synthesis. For this purpose, a microwave synthesizer was programmed to operate in a fixed temperature mode, whereby a temperature control point and a run time (time held at the specified temperature) were set, thus allowing the instrument to automatically control the power delivered to the reactor. To investigate the optimal conditions of heating, different cases were studied, whereby the reactant compositions (i.e., 0.75 mL of 10 mM $HAuCl_4$ and 5 mL of 0.1 % (w/v) chitosan solution) were the same for all cases, while the temperature and holding time varied. It was found that in all cases, the color of the reactant solution changed from yellow to colorless and eventually to ruby red within 10 s after a 1 min ramp period, indicating the formation of AuNPs. Moreover, the different reaction temperatures significantly affected the maximum wavelength and intensity of peaks in the UV–vis spectra of the products. When the reaction was allowed to proceed for 40 s, a low yield of CS-AuNPs was obtained at 105 °C (Fig. 1a), probably due to insufficient heating. When the temperature was increased to 125 °C, which would increase the reaction rate, a higher yield of CS-AuNPs was formed, and a single, intense peak with the absorption maxima at 520 nm was observed, corresponding to a deep-red solution. When the temperature was further increased to 145 °C, however, a purplish red AuNPs solution was formed, and an additional peak was observed at around 650 nm in the spectrum. In agreement with the earlier reports (Muralidharan, Subramanian, Nallamuthu, Santhanam, & Kumar, 2011), this effect was probably due to the increase in particle size caused by the agglomeration of small particles formed at a too-high temperature. As measured by dynamic light scattering (DLS), the hydrodynamic size of CS-AuNPs prepared at 145 °C was also found to be larger than those synthesized at 125 °C (Fig. 2).

When the synthesis was conducted at 125 °C under different holding times, 20–60 s, it was found that the holding time had a less pronounced effect on the UV–vis spectra compared with the temperature (Fig. 1b). Nevertheless, the prolonged heating time of 90 s led to the aggregation and settling down of the particles in the synthesis vessel, resulting in a loss in yield. However, the reaction maintained for 40 s resulted in a UV–vis spectrum with a narrower surface plasmon resonance band in the shorter (bluer) wavelengths, which indicates a smaller particle size. In addition, the particle size distribution was more uniform than the others, as analyzed by DLS (Fig. 2). Therefore, the optimal conditions for the synthesis of CS-AuNPs in this study were a temperature of 125 °C and a heating time of 40 s.

3.2. Characteristics of CS-AuNPs

The solution of CS-AuNPs prepared using the optimal reaction conditions exhibited a red color with an absorption band at 520 nm. The colloidal property was confirmed by the observation of the Tyndall

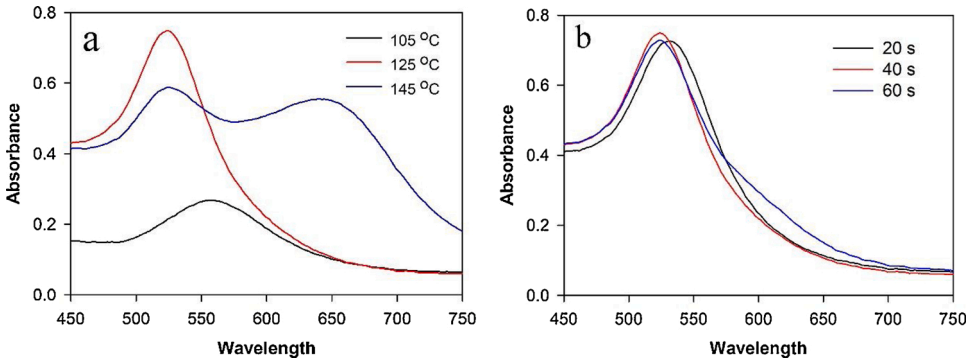

Fig. 1. UV–vis spectra of CS-AuNPs prepared under different (a) reaction temperatures (time = 40 s) and (b) times (temperature =125 °C).

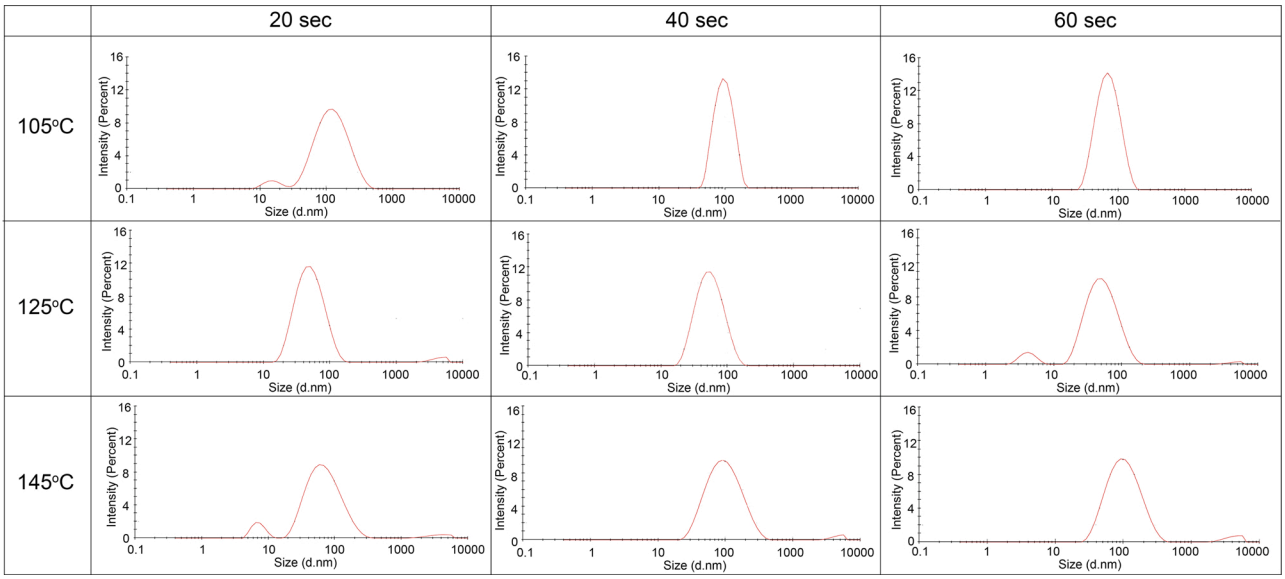

Fig. 2. Particle size distribution of CS-AuNPs prepared under different reaction temperatures (rows) and times (column) as determined by DLS technique.

effect. The CS-AuNPs had a spherical shape with an average diameter of 17.8 ± 3.9 nm, as determined by TEM. The hydrodynamic diameter obtained from DLS experiments was 43.8 nm, with a polydispersity index of 0.32. The difference in particle size, estimated by the two abovementioned techniques, may be attributed to the high swelling capability of the chitosan polymer coating on the particles. As the synthesis was performed in an acidic medium, chitosan molecules containing amine groups underwent protonation, thus producing CS-AuNPs having a positive zeta potential of about 30 mV on their surface.

Fig. 3 displays the FTIR spectrum of pure chitosan, which presented a broad band at 3421 cm^{-1}, due to stretching vibrations overlapping between O–H and N–H groups. The peak at 2923 cm^{-1}represents the stretching of C–H. The bands located at 1646 cm^{-1} (stretching vibrations of C = O) indicated the presence of carbonyl groups. The peak at

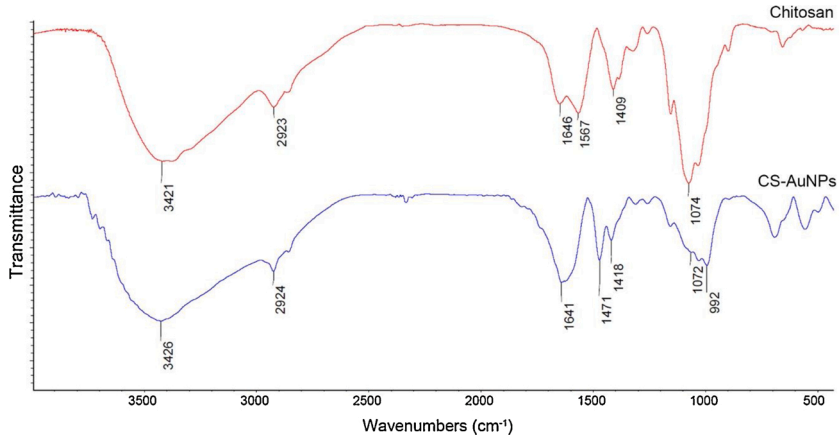

Fig. 3. FTIR spectra of (a) chitosan (red line) and (b) CS-AuNPs (blue line).

1567 and 1409 cm^{-1}corresponds to N–H bending vibration in amine, and the band at 1074 cm^{-1} is attributed to the C – O stretching of glycosidic linkage. Furthermore, for the FTIR spectrum of CS-AuNPs, most of the bands were similar to those of chitosan. The band at 1641 cm^{-1}, representing C = O stretching vibration, has a higher intensity than that of chitosan, due to the oxidation of hydroxyl groups in chitosan by Au^{3+} to carbonyl functional groups. The band at 1567 cm^{-1} in chitosan spectrum was shifted to 1471 cm^{-1}which indicated that the AuNPs bound to chitosan through affinity interaction with amino groups, thus decreasing the vibration of N–H bond (Komalam et al., 2012; Wei & Qian, 2006). Moreover, the C–O stretching band of CS-AuNPs at 1072 cm^{-1} had a lower intensity than that of chitosan, due to the hydrolysis of partial glycosidic linkages during the synthesis reaction (Pestov, Nazirov, Modin, Mironenko, & Bratskaya, 2015).

The analysis of ^{1}H NMR spectroscopy of CS-AuNPs fabricated by microwave irradiation in this work revealed that the ratio of integral intensities of signals H atoms at 2.06 ppm (CH_3) and 3.23 ppm (H-2) of CS-AuNPs (1.12) was lower than that of original chitosan (2.50), indicating that the deacetylation occurred (Fig. 4). Besides, the chitosan chain was hydrolyzed as evidenced by the presence of a signal corresponding to the H-atom in hemiacetal group at 5.45 ppm in CS-AuNPs and a remarkable decrease of the solution viscosity due to shortening of chitosan chain from 12.61 $\pm$ 0.19 cP of original chitosan solution to 4.94 $\pm$ 0.02 cP of CS-AuNPs solution. These results supported that the reaction with Au(III) led to the hydrolysis and chain fragmentation/opening of chitosan and its products act as the main reducing species. This finding was in agreement with the mechanism proposed by Pestov et al. (2015)

As reported by other works, the hydrolysis of chitosan in an acidic electrolyte solution was also observed upon the microwave irradiation. As a result, microwave heating is used as an effective tool for the preparation of low molecular weight and oligomeric chitosan since it is capable of accelerating the hydrolytic deacetylation and depolymerization of chitosan (Heng, Yuguang, & Junzeng, 2009; Sahu, Goswami, & Bora, 2009; Xing et al., 2004). Especially, in the presence of inorganic halide salts such as NaCl, KCl and $MgCl_2$ the hydrolysis rate was greatly improved, probably through the increase of solution conductivity as well as the enhancement of dielectric effects and microwave coupling of the solvents (Ali et al., 2015). Furthermore, for the synthesis of other metal nanoparticles e.g. silver nanoparticles, microwave irradiation is also an attractive alternative to conventional, convective heating due to the effects of efficient heating as well as microwave effects, i.e., those resulting from the material and wave interactions and the dipolar polarization phenomenon (Dahal, García, Zhou, & Humphrey, 2012; Das, Mukhopadhyay, Datta, & Basu, 2009; Gawande, Shelke, Zboril, & Varma, 2014). Taken together, it is hypothesized that rapid and uniform microwave heating enable fast and efficient synthesis of CS-AuNPs by accelerating the hydrolysis of chitosan to active reducing species and promoting homogeneous nucleation and growth of CS-AuNPs.

In terms of stability, no significant change was observed after the CS-AuNPs were kept at 4 °C for 21 days. Hence, green and naturally derived chitosan could effectively act as both a reducing agent and a stabilizing agent and the synthesis route proposed in this study may be employed to fabricate CS-AuNPs for other applications. However, it should be noted that even though chitosan is generally considered biocompatible, by-products such as formic acid are generated upon chitosan hydrolysis and oxidation with Au(III) during the synthesis of CS-AuNPs (Nazirov et al., 2016; Pestov et al., 2015; Silvestri et al., 2018). Consequently, the extent of such by-products should be considered to ensure that CS-AuNPs are safe when used for biomedical applications.

3.3. Analytical applicability of CS-AuNPs

3.3.1. Principle of the colorimetric assay of Na_2EDTA

The NH_3^+ in CS-AuNPs can react with polyanionic compounds through electrostatic interaction and induce the aggregation of AuNPs, leading to a red-to-blue color change; this property can be employed for the development of colorimetric assays for this type of analytes. The compound EDTA, used as an antidote for heavy metals, contains polycarboxylic groups. The pharmacopeial assay method used for the quality control of Na_2EDTA injection in UV–vis pharmaceutical manufacturing relies on a complexometric titration method that consists of several steps, consumes large amounts of reagents, and does not enable the simultaneous analysis of multiple samples. To overcome these drawbacks and demonstrate the analytical applicability of CS-AuNPs, in this study, a new method in which CS-AuNPs are used as the colorimetric sensor was developed for the assay of disodium edetate intravenous injections. The reaction in which Na_2EDTA induced the aggregation of CS-AuNPs is shown in Fig. 5. This aggregation resulted in a colorimetric response (changing from red to blue) corresponding to a shift of the surface plasmon resonance band from 520 to 670 nm (Fig. 6a). The aggregation of CS-AuNPs was confirmed by TEM photographs (Fig. 6b–c).

3.3.2. Optimal conditions for the assay

3.3.2.1. pH of the reaction. The optimal condition for the assay was initially investigated by selecting the pH at which CS-AuNPs were stable. The CS-AuNPs were incubated in the buffer under different pH conditions, and the red color of CS-AuNPs solution gradually turned purple as the pH increased above 5. This observation corresponded to the increase in absorbance at 670 nm (Fig. 7a). With a pK_a of 6.5, chitosan is soluble and exists as a cationic polymer in aqueous medium below pH 6.5. When the pH was above the pK_a value, chitosan had limited water solubility

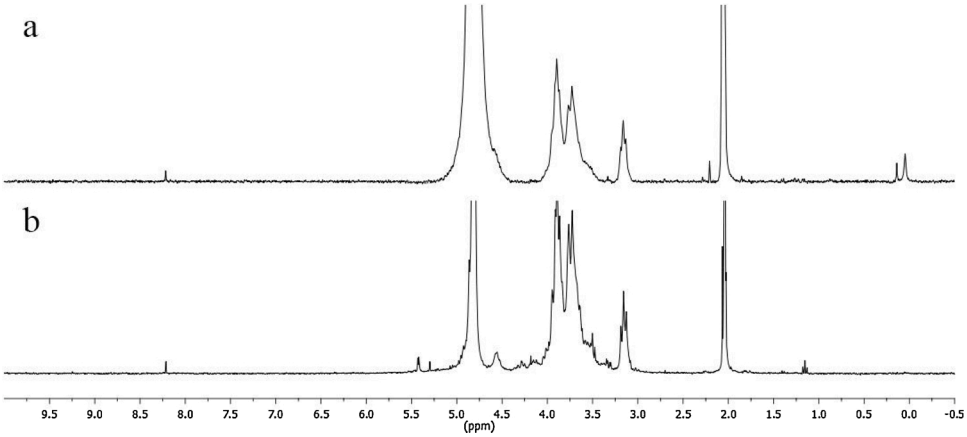

Fig. 4. ^{1}H NMR spectra of chitosan (a) and CS-AuNPs (b).

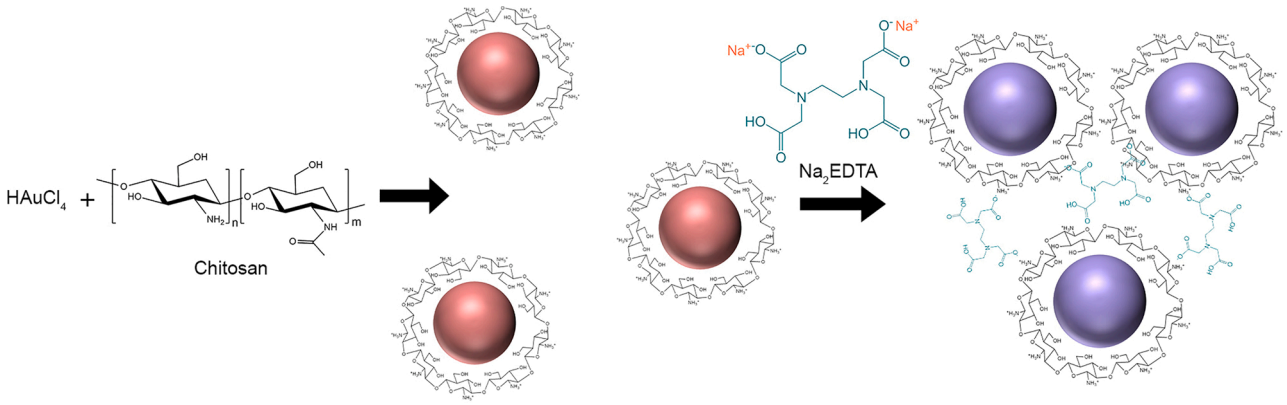

Fig. 5. Proposed mechanism of colorimetric reaction between CS-AuNPs and Na_2EDTA.

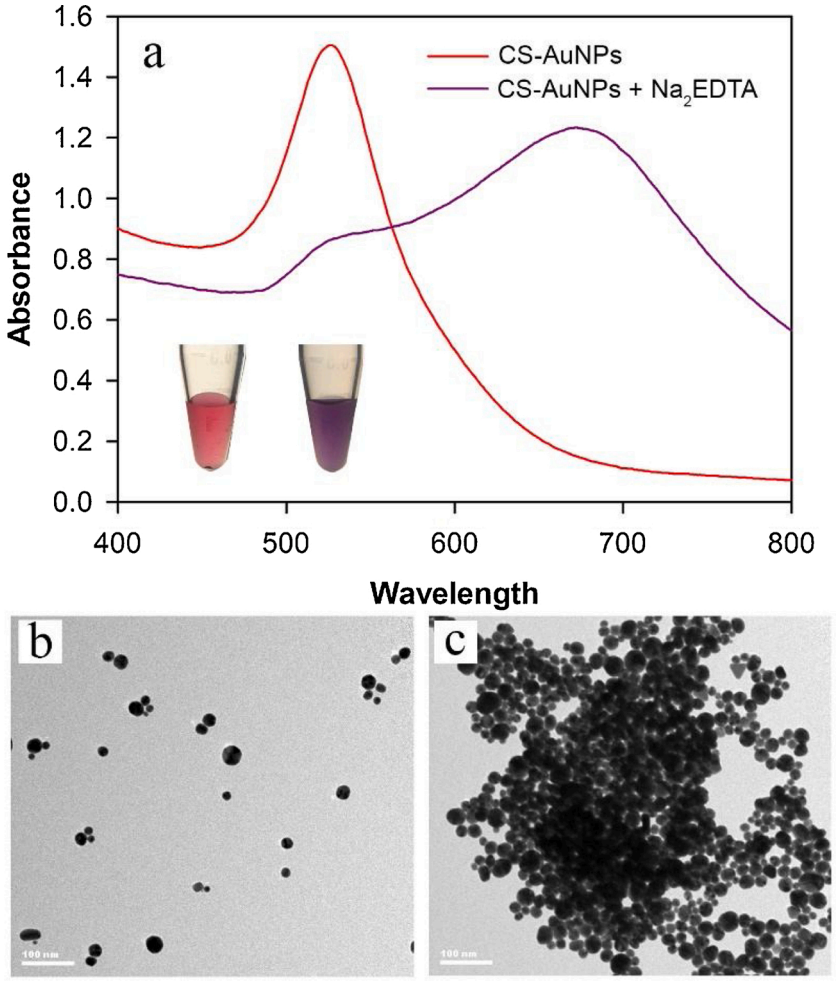

Fig. 6. (a) UV–vis spectra of CS-AuNPs before (red line) and after (purple line) the addition of Na_2EDTA; TEM images of (b) CS-AuNPs and (c) aggregate CS-AuNPs.

and precipitated and thus could not efficiently stabilize the AuNPs, leading to the formation of large aggregates of AuNPs. Since the CS-AuNPs solution color began to change without induction by Na_2EDTA at pH $\geq$ 5, this pH range was improper for the assay.

When the effects of pH 2 to 4 on the reaction involving Na_2EDTA were further studied, the results showed that pH 4 was the most effective since it gave a standard curve in which the absorbance significantly responded to the analyte concentration (Fig. 7b). At pH $\leq$ 3 where EDTA became protonated, negatively charged species of EDTA were available at a low amount to react with CS-AuNPs. Therefore, the color change was very low and unnoticeable under this condition.

3.3.2.2. Volume of CS-AuNPs solution. The AuNPs concentration is another parameter that should be considered to improve the sensitivity of the method; different volumes of the as-prepared CS-AuNPs solution were thus tested for use in the assay conducted at pH 4. As shown in Fig. 7c, increasing the volume of CS-AuNPs from 50 to 100 μL resulted in an increment in the absorbance values and the slope of the standard curve, indicating the higher sensitivity of the method. The increase in the CS-AuNPs volume to 150 μL, however, did not further improve the

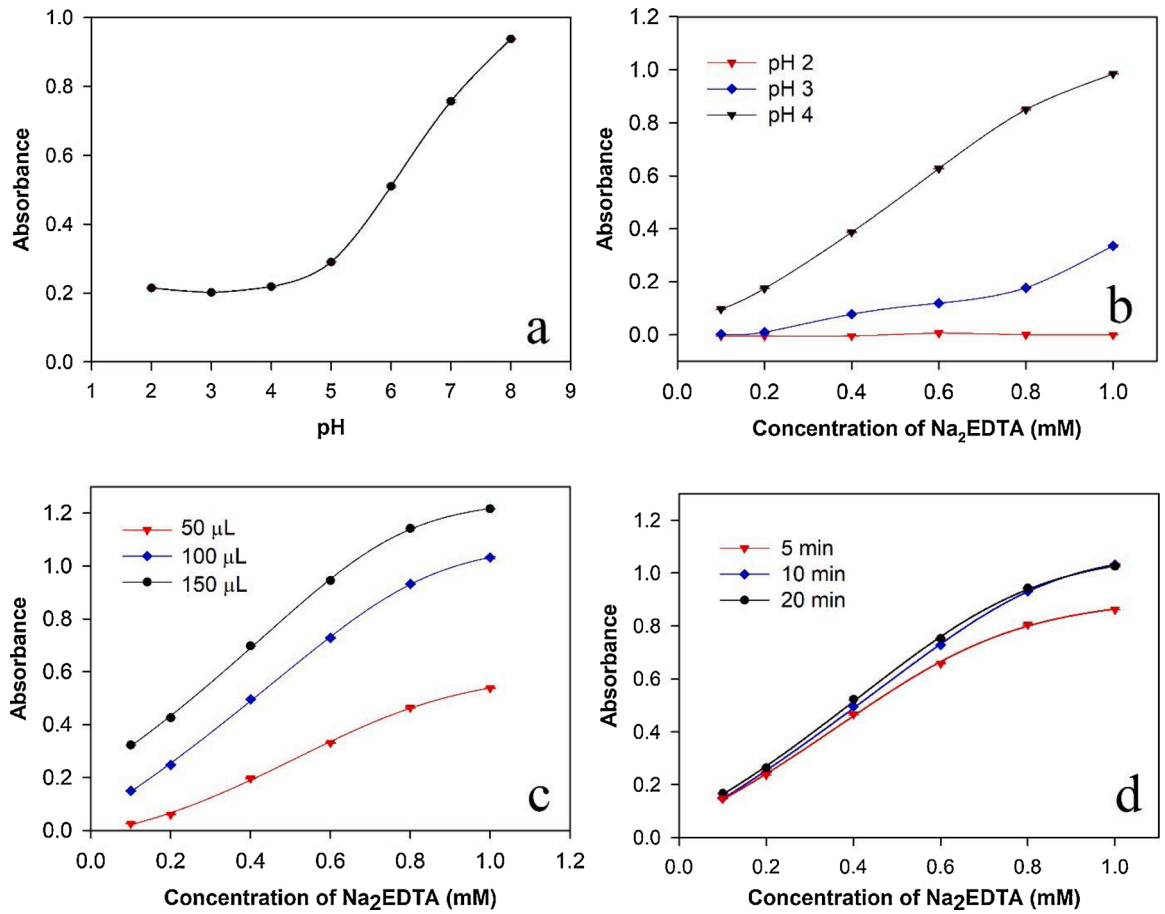

Fig. 7. (a) Effect of pH on absorbance at 670 nm of CS-AuNPs and effects of (b) pH, (c) volume of CS-AuNPs, and (d) assay reaction time on the plots of absorbance at 670 nm versus Na_2EDTA concentration.

sensitivity; the corresponding curve was parallel to that of 100 µL. Considering the above results, 100 µL was chosen as the optimal volume of CS-AuNPs solution, which benefited from both satisfactory sensitivity and cost saving through the use of minimal amounts of reagents.

3.3.2.3. Reaction time. Since the aggregation of CS-AuNPs induced by Na_2EDTA required several minutes to complete, the shortest reaction time that produced the most intense solution color was investigated. As shown in Fig. 7d, when the reaction was allowed to occur for 5 min, the obtained standard curve was lower than those of the other reaction times, because the reaction was not yet completed. By incubating the reaction of CS-AuNPs and Na_2EDTA for a longer time, the curves of 10 and 20 min reaction times showed higher absorbance values than that of the 5 min curve. Moreover, the 10 and 20 min curves were not significantly different; implying that the detection could be readily performed after the assay reaction was incubated for 10 min. In addition, the color developed was stable for at least 20 min. Nevertheless, when the reaction was left for more than 1 h, the solution color began to fade due to the precipitation of the aggregate particles. Thus, it is recommended that the absorbance be read within 10–20 min after all reagents are mixed in the reaction.

3.3.3. Analytical performance of the assay

After the assay conditions were optimized, the method was validated. To establish the relationship between the analytical signal, i.e., the absorbance at 670 nm and the concentration of Na_2EDTA, an appropriate regression equation was investigated. In our case, a simple linear regression was unlikely to be the best model since the standard curve produced an S-shaped sigmoidal relationship; therefore, a nonlinear regression model was more suitable. The obtained response relationship is similar to those of numerous biological assays; for example, immunoassays, dose-response curves, and ligand binding assays do not follow a linear response; therefore, logistic regression models such as the 4-parameter logistic (4 PL) (Sameenoi, Mensack, Murphy, & Henry, 2012) and 5-parameter logistic (van Gageldonk, van Schaijk, van der Klis, & Berbers, 2008) are generally necessary and recommended. Since the standard curve of the proposed assay was symmetrical and S-shaped (Fig. 8), it agrees well with a 4 PL regression equation, as shown below, and this model was therefore chosen for the determination of Na_2EDTA in a concentration range of 0.1–1.2 mM.

$$y = \min + \frac{(\max - \min)}{1 + \left(\frac{x}{EC_{50}}\right)^{-Hillslope}}$$

where y is the absorbance at 670 nm and x is the concentration of Na_2EDTA (mM); min = 0.0910, max = 1.2792, EC_{50} = 0.6386, and Hillslope = 2.3777

From the regression analysis, the coefficient of determination R^2 was obtained as 0.9992, which is very close to 1, in the analyte concentration range of 0.1–1.2 mM. In addition, other regression parameters, including the mean square error (0.0003), the sum of squared residuals (0.0008), and the standard deviation of the residuals (0.0163) were all close to 0. Taken together, these results demonstrate the goodness of fit of the 4 PL model, so this model was chosen for the determination of Na_2EDTA using the proposed assay. Although the nonlinear 4 PL was more complicated than a linear model, in practice, curve fitting and calculation of the assay results can be conveniently done using software programs, such as SigmaPlot and Assayfit Pro, a Microsoft Excel add-in,

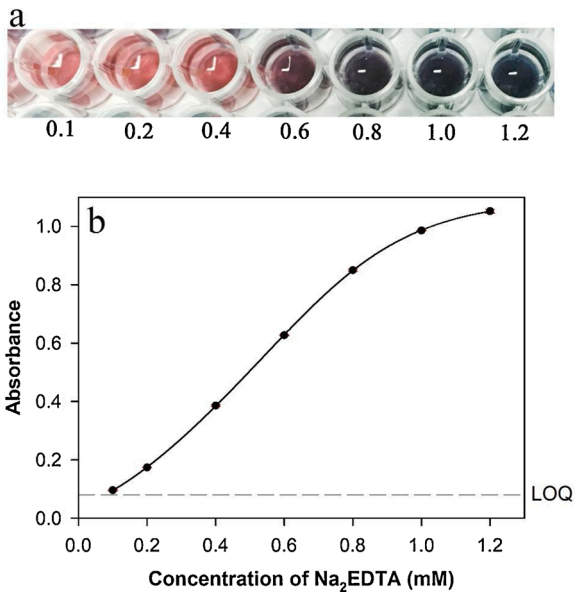

Fig. 8. (a) Photograph of the colorimetric assay reaction in the presence of 0.1–1.2 mM Na_2EDTA and (b) a 4-parameter logistic standard curve showing LOQ at 0.080 mM Na_2EDTA.

or free online curve-fitting tools, such as MyCurveFit.com and MyAssays.com.

From the standard curve, the LOD and LOQ for the determination of Na_2EDTA were found to be 0.036 and 0.080 mM, respectively. The method was accurate as confirmed by the percent recovery values of 99.2%, 100.8%, and 101.6% (n = 3) for the 3 levels of Na_2EDTA concentration, i.e., 0.4, 0.5 and 0.6 mM, respectively. The precision studies performed with 6 independent assays revealed the % RSD values of 1.1 and 1.47 for the intra-day and inter-day precision, respectively, indicating acceptable reproducibility and repeatability. However, although the specificity of the method was not studied in this work since the injection contained only Na_2EDTA, this parameter needs to be validated if CS-AuNPs are used for the assays of samples containing a more complex matrix. Lastly, the proposed method was used for the assay of the commercial disodium edetate injections in comparison with the USP titrimetric method. The % labeled amounts of drug (n = 6) assayed by the CS-AuNPs method and the reference method were 100.67 ± 0.68 % and 100.36 ± 0.28 %, respectively. According to the Student's *t*-test at 95% confidence level, these results were not significantly different (the calculated and critical t-values were 1.018 and 2.365, respectively). Considering the above results, the developed method is feasible for the quality control of disodium edetate injections. It is more suitable for the analysis of large numbers of samples than titration and also offers the possibility of automation. Moreover, the method may be further applied to the analysis of other polyanionic substances.

3.4. Laboratory waste treatment and gold recovery

In present times, the environmental impacts and toxicity of metal nanoparticles have gained much attention because of the increasing use and release of these nanomaterials into the environment. The toxicity of AuNPs, although considered low, is likely caused by the ligands rather than the particles themselves (Zhang et al., 2019). However, an increasing number of studies have revealed the potential environmental impact of AuNPs, especially on aquatic organisms as many discarded products and wastes containing AuNPs end up in waterways. For instance, Dedeh et al. reported that exposure to AuNPs triggered modifications of genome composition and gene expression in fish tissues. In addition, AuNPs have been found to alter neurotransmission by increasing fish brain acetylcholine esterase activity; this was not observed for ionic gold, thereby underlining the higher toxic potential of the nanoparticle form (Dedeh, Ciutat, Treguer-Delapierre, & Bourdineaud, 2015). Even chitosan, which was used as a capping agent in this work, is considered a nontoxic green material. However, the safety issue of gold nanoparticles to the environment and human health is still controversial, and therefore, the release or disposal of CS-AuNPs deserves more caution to minimize potential hazards.

Given that CS-AuNPs precipitate at the pH above 6.5, wastes generated from the assays in this work were treated by adjusting the pH to 7 in order to transform the nanoparticles into the large aggregates easily removable by centrifugation. This method was proved to be effective since most CS-AuNPs in the waste, including the products formed between CS-AuNPs and Na_2EDTA as well as the residual unreacted CS-AuNPs, were sedimented from the initial purple-colored waste solution, yielding a nearly colorless supernatant. Surprisingly, after centrifugation, a layer of shiny gold precipitate co-existing with dark-colored powders was obtained (Fig. 9a, left tube). This phenomenon was unique to CS-AuNPs and was not seen in the precipitate of citrate-capped AuNPs obtained by adjusting the solution pH to a much higher level than 7 in order to induce sedimentation (Fig. 9a, right tube). The results imply that compared with citrate ion, chitosan was bound to AuNPs with a weaker affinity as it easily separated from the gold surface when the solution pH was 7.

To further refine the gold, the dried precipitate of CS-AuNPs was digested by acid and then ignited to get rid of organic matter as well as the synthesis by-products e.g. formic acid. The photograph of the recovered gold is displayed in Fig. 9b, and the SEM-EDS analysis result (Fig. 9b–c) confirmed the identity of gold and indicated a purity of 97.62% by weight. This study not only offers a simple and effective laboratory method for treating CS-AuNPs-containing waste but also reports for the first time the distinctive feature of CS-AuNPs useful for gold recovery. Therefore, CS-AuNP is an intriguing material whose waste can be easily managed and recycled as high-value metal, promoting both environmental sustainability and economic feasibility.

4. Conclusion

A CS-AuNPs synthesis method using chitosan as both a reducing and a stabilizing agent was investigated. Microwave irradiation under a fixed temperature mode, which has never been reported was employed as the heating method. The CS-AuNPs with desirable size, monodispersity, and light absorption properties were obtained in less than 2 min. Due to the positively charged surface, CS-AuNPs were utilized for the assay of disodium edetate in injection based on the aggregation-induced color change. Compared with the currently used titrimetric method, the proposed validated method was simpler, rapid, required fewer reagents, and suitable for the analysis of a large number of samples. Based on this feature a straightforward laboratory technique was employed to effectively turn the CS-AuNPs waste into an environmentally friendly and economically beneficial product.

CRediT authorship contribution statement

Thana Thanayutsiri: Conceptualization, Methodology, Investigation, Writing - original draft, Visualization. **Prasopchai Patrojanasophon:** Formal analysis. **Praneet Opanasopit:** Formal analysis. **Tanasait Ngawhirunpat:** Formal analysis. **Samawadee Plianwong:** Investigation, Resources. **Theerasak Rojanarata:** Conceptualization, Methodology, Investigation, Formal analysis, Writing - review & editing, Supervision, Project administration, Funding acquisition.

Declaration of Competing Interest

The authors declare that there is no conflict of interest.

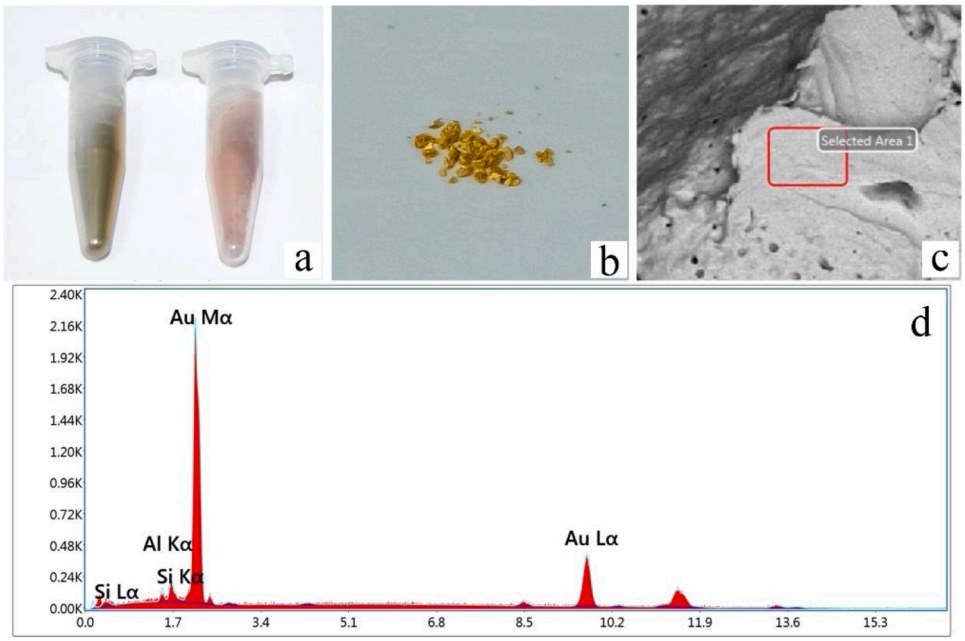

Fig. 9. (a) Photographs of dried precipitates of CS-AuNPs (left tube) and citrate-capped AuNPs (right tube) after alkaline treatment; (b) gold refined after removal of organic matter by acid digestion and heating; (c) SEM micrograph (top view) of gold grain; (d) EDS spectra of gold within the representative microscopic area marked with red-bordered rectangle in (c).

Acknowledgements

The authors gratefully acknowledge the financial support from Thailand Research Fund (TRF) through the Royal Golden Jubilee Ph.D. Program Scholarship Grant No. PHD/0142/2560 for Thana Thanayutsiri. We also thank John Tigue, Ph.D., for his valuable help in editing and proofreading the manuscript.

References

Abrica-González, P., Zamora-Justo, J. A., Sotelo-López, A., Vázquez-Martínez, G. R., Balderas-López, J. A., Muñoz-Diosdado, A., et al. (2019). Gold nanoparticles with chitosan, N-acylated chitosan, and chitosan oligosaccharide as DNA carriers. *Nanoscale Research letters, 14*(1), 258.

Akshaya, K., Arthi, C., Pavithra, A. J., Poovizhi, P., Antinate, S. S., Hikku, G. S., et al. (2020). Bioconjugated gold nanoparticles as an efficient colorimetric sensor for cancer diagnostics. *Photodiagnosis and Photodynamic Therapy, 30*, Article 101699.

Ali, K., Ahmed, B., Dwivedi, S., Saquib, Q., Al-Khedhairy, A. A., & Musarrat, J. (2015). Microwave accelerated green synthesis of stable silver nanoparticles with eucalyptus globulus leaf extract and their antibacterial and antibiofilm activity on clinical isolates. *PLOS ONE, 10*(7), Article e0131178.

Augustine, R., & Hasan, A. (2020). Emerging applications of biocompatible phytosynthesized metal/metal oxide nanoparticles in healthcare. *Journal of Drug Delivery Science and Technology, 56*, Article 101516.

Bu, T., Zhang, M., Sun, X., Tian, Y., Bai, F., Jia, P., et al. (2019). Gold nanoparticles-functionalized microorganisms assisted construction of immunobiosensor for sensitive detection of ochratoxin A in food samples. *Sensors and Actuators B: Chemical, 299*, Article 126969.

Chen, X., Zhao, X., Gao, Y., Yin, J., Bai, M., & Wang, F. (2018). Green synthesis of gold nanoparticles using carrageenan oligosaccharide and their in vitro antitumor activity. *Marine drugs, 16*(8), 277.

Chen, Z., Wang, Z., Chen, X., Xu, H., & Liu, J. (2013). Chitosan-capped gold nanoparticles for selective and colorimetric sensing of heparin. *Journal of Nanoparticle Research, 15*(9), 1930.

Dahal, N., García, S., Zhou, J., & Humphrey, S. M. (2012). Beneficial effects of microwave-assisted heating versus conventional heating in noble metal nanoparticle synthesis. *ACS Nano, 6*(11), 9433–9446.

Das, S., Mukhopadhyay, A. K., Datta, S., & Basu, D. (2009). Prospects of microwave processing: An overview. *Bulletin of Materials Science, 32*(1), 1–13.

Dedeh, A., Ciutat, A., Treguer-Delapierre, M., & Bourdineaud, J.-P. (2015). Impact of gold nanoparticles on zebrafish exposed to a spiked sediment. *Nanotoxicology, 9*(1), 71–80.

Devendiran, R. M., Chinnaiyan, S. k., Yadav, N. K., Moorthy, G. K., Ramanathan, G., Singaravelu, S., et al. (2016). Green synthesis of folic acid-conjugated gold nanoparticles with pectin as reducing/stabilizing agent for cancer theranostics. *RSC Advances, 6*(35), 29757–29768.

Dhar, S., Mali, V., Bodhankar, S., Shiras, A., Prasad, B. L. V., & Pokharkar, V. (2011). Biocompatible gellan gum-reduced gold nanoparticles: cellular uptake and subacute oral toxicity studies. *Journal of Applied Toxicology, 31*(5), 411–420.

El-Naggar, M. E., Shaheen, T. I., Fouda, M. M. G., & Hebeish, A. A. (2016). Eco-friendly microwave-assisted green and rapid synthesis of well-stabilized gold and core–shell silver–gold nanoparticles. *Carbohydrate Polymers, 136*, 1128–1136.

Fan, C., Li, W., Zhao, S., Chen, J., & Li, X. (2008). Efficient one pot synthesis of chitosan-induced gold nanoparticles by microwave irradiation. *Materials Letters, 62*(20), 3518–3520.

Gawande, M. B., Shelke, S. N., Zboril, R., & Varma, R. S. (2014). Microwave-assisted chemistry: synthetic applications for rapid assembly of nanomaterials and organics. *Accounts of Chemical Research, 47*(4), 1338–1348.

Heng, Y., Yuguang, D., & Junzeng, Z. (2009). Low molecular weight and oligomeric chitosans and their bioactivities. *Current Topics in Medicinal Chemistry, 9*(16), 1546–1559.

Huang, H., & Yang, X. (2004). Synthesis of chitosan-stabilized gold nanoparticles in the absence/presence of tripolyphosphate. *Biomacromolecules, 5*(6), 2340–2346.

ICH Q2 (R1). (2005). *Validation of analytical procedures (definitions and terminology)*.

Jiang, C., Zhu, J., Li, Z., Luo, J., Wang, J., & Sun, Y. (2017). Chitosan–gold nanoparticles as peroxidase mimic and their application in glucose detection in serum. *RSC Advances, 7*(70), 44463–44469.

Kalimuthu, K., Cha, B. S., Kim, S., & Park, K. S. (2020). Eco-friendly synthesis and biomedical applications of gold nanoparticles: A review. *Microchemical Journal, 152*, Article 104296.

Kattumuri, V., Chandrasekhar, M., Guha, S., Raghuraman, K., Katti, K. V., Ghosh, K., et al. (2006). Agarose-stabilized gold nanoparticles for surface-enhanced Raman spectroscopic detection of DNA nucleosides. *Applied Physics Letters, 88*(15), Article 153114.

Khan, T., Ullah, N., Khan, M. A., Mashwani, Z.-u.-R., & Nadhman, A. (2019). Plant-based gold nanoparticles; a comprehensive review of the decade-long research on synthesis, mechanistic aspects and diverse applications. *Advances in Colloid and Interface Science, 272*, Article 102017.

Kim, H., Nguyen, V. P., Manivasagan, P., Jung, M. J., Kim, S. W., Oh, J., et al. (2017). Doxorubicin-fucoidan-gold nanoparticles composite for dual-chemo-photothermal treatment on eye tumors. *Oncotarget, 8*(69), 113719–113733.

Komalam, A., Muraleegharan, L. G., Subburaj, S., Suseela, S., Babu, A., & George, S. (2012). Designed plasmonic nanocatalysts for the reduction of eosin Y: absorption and fluorescence study. *International Nano Letters, 2*(1), 26.

Kumari, K. A., Reddy, G. B., & Mittapalli, V. (2020). Microwave assisted synthesis of gold nanoparticles with Phyla nodiflora (L.) Greene leaves extract and its studies of catalytic reduction of organic pollutants. *Materials Today: Proceedings*.

Latif, M. S., Kormin, F., Mustafa, M. K., Mohamad, I. I., Khan, M., Abbas, S., et al. (2018). Effect of temperature on the synthesis of Centella asiatica flavonoids extract-mediated gold nanoparticles: UV-visible spectra analyses. *AIP Conference Proceedings, 2016*(1), Article 020071.

Lim, E.-K., Jang, E., Kim, J., Lee, T., Kim, E., Park, H. S., et al. (2012). Self-fabricated dextran-coated gold nanoparticles using pyrenyl dextran as a reducible stabilizer and their application as CT imaging agents for atherosclerosis. *Journal of Materials Chemistry, 22*(34), 17518–17524.

Liu, B., & Liu, J. (2019). Interface-Driven Hybrid Materials Based on DNA-Functionalized Gold Nanoparticles. *Matter, 1*(4), 825–847.
Madhavan, V., Gangadharan, P. K., Ajayan, A., Chandran, S., & Raveendran, P. (2019). Microwave-assisted solid-state synthesis of Au nanoparticles, size-selective speciation, and their self-assembly into 2D-superlattice. *Nano-Structures & Nano-Objects, 17*, 218–222.
Manivasagan, P., Bharathiraja, S., Bui, N. Q., Lim, I. G., & Oh, J. (2016). Paclitaxel-loaded chitosan oligosaccharide-stabilized gold nanoparticles as novel agents for drug delivery and photoacoustic imaging of cancer cells. *International Journal of Pharmaceutics, 511*(1), 367–379.
Martínez-Torres, A. C., Zarate-Triviño, D. G., Lorenzo-Anota, H. Y., Ávila-Ávila, A., Rodríguez-Abrego, C., & Rodríguez-Padilla, C. (2018). Chitosan gold nanoparticles induce cell death in HeLa and MCF-7 cells through reactive oxygen species production. *International Journal of Nanomedicine, 13*, 3235–3250.
Mohan, C. O., Gunasekaran, S., & Ravishankar, C. N. (2019). Chitosan-capped gold nanoparticles for indicating temperature abuse in frozen stored products. *npj Science of Food, 3*(1), 2.
Morad, M., Karim, M. A., Altass, H. M., & Khder, A. E. R. S. (2019). Microwave-assisted synthesis of gold nanoparticles supported on Mn 3 O 4 catalyst for low temperature CO oxidation. *Environmental Technology*, 1–10.
Muralidharan, G., Subramanian, L., Nallamuthu, S. K., Santhanam, V., & Kumar, S. (2011). Effect of reagent addition rate and temperature on synthesis of gold nanoparticles in microemulsion route. *Industrial & Engineering Chemistry Research, 50*(14), 8786–8791.
Nazirov, A., Pestov, A., Privar, Y., Ustinov, A., Modin, E., & Bratskaya, S. (2016). One-pot green synthesis of luminescent gold nanoparticles using imidazole derivative of chitosan. *Carbohydrate Polymers, 151*, 649–655.
Patil, M. P., & Kim, G.-D. (2018). Marine microorganisms for synthesis of metallic nanoparticles and their biomedical applications. *Colloids and Surfaces B: Biointerfaces, 172*, 487–495.
Pestov, A., Nazirov, A., Modin, E., Mironenko, A., & Bratskaya, S. (2015). Mechanism of Au(III) reduction by chitosan: Comprehensive study with ^{13}C and ^{1}H NMR analysis of chitosan degradation products. *Carbohydrate Polymers, 117*, 70–77.
Potara, M., Maniu, D., & Astilean, S. (2009). The synthesis of biocompatible and SERS-active gold nanoparticles using chitosan. *Nanotechnology, 20*(31), Article 315602.
Rovais, M. R. A., Alirezapour, B., Moassesi, M. E., Amiri, M., Novin, F. B., & Maadi, E. (2018). Internalization capabilities of gold-198 nanoparticles: Comparative evaluation of effects of chitosan agent on cellular uptake into MCF-7. *Applied Radiation and Isotopes, 142*, 85–91.
Sahu, A., Goswami, P., & Bora, U. (2009). Microwave mediated rapid synthesis of chitosan. *Journal of Materials Science: Materials in Medicine, 20*(1), 171–175.
Salem, D. S., Sliem, M. A., El-Sesy, M., Shouman, S. A., & Badr, Y. (2018). Improved chemo-photothermal therapy of hepatocellular carcinoma using chitosan-coated gold nanoparticles. *Journal of Photochemistry and Photobiology B: Biology, 182*, 92–99.
Sameenoi, Y., Mensack, M. M., Murphy, B. M., & Henry, C. S. (2012). Competitive, non-competitive, and mixed format cleavable tag immunoassays. *Methods, 56*(2), 166–173.
Santhoshkumar, J., Rajeshkumar, S., & Venkat Kumar, S. (2017). Phyto-assisted synthesis, characterization and applications of gold nanoparticles – A review. *Biochemistry and Biophysics Reports, 11*, 46–57.
Shrivas, K., Nirmalkar, N., Thakur, S. S., Deb, M. K., Shinde, S. S., & Shankar, R. (2018). Sucrose capped gold nanoparticles as a plasmonic chemical sensor based on non-covalent interactions: Application for selective detection of vitamins B1 and B6 in brown and white rice food samples. *Food Chemistry, 250*, 14–21.
Silvestri, D., Wacławek, S., Sobel, B., Torres-Mendieta, R., Novotný, V., Nguyen, N. H. A., et al. (2018). A poly(3-hydroxybutyrate)–chitosan polymer conjugate for the synthesis of safer gold nanoparticles and their applications. *Green Chemistry, 20*(21), 4975–4982.
Sonia, Komal, Kukreti, S., & Kaushik, M. (2018). Exploring the DNA damaging potential of chitosan and citrate-reduced gold nanoparticles: Physicochemical approach. *International Journal of Biological Macromolecules, 115*, 801–810.
Sun, I.-C., Ahn, C.-H., Kim, K., & Emelianov, S. (2019). Photoacoustic imaging of cancer cells with glycol-chitosan-coated gold nanoparticles as contrast agents. *Journal of Biomedical Optics, 24*(12), Article 121903.
Sun, L., Li, J., Cai, J., Zhong, L., Ren, G., & Ma, Q. (2017). One pot synthesis of gold nanoparticles using chitosan with varying degree of deacetylation and molecular weight. *Carbohydrate Polymers, 178*, 105–114.
Suvarna, S., Das, U., Kc, S., Mishra, S., Sudarshan, M., Saha, K. D., et al. (2017). Synthesis of a novel glucose capped gold nanoparticle as a better theranostic candidate. *PLOS ONE, 12*(6), Article e0178202.
Teimouri, M., Khosravi-Nejad, F., Attar, F., Saboury, A. A., Kostova, I., Benelli, G., et al. (2018). Gold nanoparticles fabrication by plant extracts: synthesis, characterization, degradation of 4-nitrophenol from industrial wastewater, and insecticidal activity – A review. *Journal of Cleaner Production, 184*, 740–753.
Tran, M., DePenning, R., Turner, M., & Padalkar, S. (2016). Effect of citrate ratio and temperature on gold nanoparticle size and morphology. *Materials Research Express, 3*(10), Article 105027.
USP43-NF38. (2020). *United States Pharmacopeia and the National Formulary*. Rockville, MD: United Book Press Inc.
van Gageldonk, P. G. M., van Schaijk, F. G., van der Klis, F. R., & Berbers, G. A. M. (2008). Development and validation of a multiplex immunoassay for the simultaneous determination of serum antibodies to Bordetella pertussis, diphtheria and tetanus. *Journal of Immunological Methods, 335*(1), 79–89.
Wei, D., & Qian, W. (2006). Chitosan-mediated synthesis of gold nanoparticles by uv photoactivation and their characterization. *Journal of nanoscience and nanotechnology, 6*, 2508–2514.
Wongmanee, K., Khuanamkam, S., & Chairam, S. (2017). Gold nanoparticles stabilized by starch polymer and their use as catalyst in homocoupling of phenylboronic acid. *Journal of King Saud University - Science, 29*(4), 547–552.
Xing, R., Liu, S., Yu, H., Zhang, Q., Li, Z., & Li, P. (2004). Preparation of low-molecular-weight and high-sulfate-content chitosans under microwave radiation and their potential antioxidant activity in vitro. *Carbohydrate research, 339*(15), 2515–2519.
Zhang, M., Yang, J., Cai, Z., Feng, Y., Wang, Y., Zhang, D., et al. (2019). Detection of engineered nanoparticles in aquatic environments: current status and challenges in enrichment, separation, and analysis. *Environmental Science: Nano, 6*(3), 709–735.